Energy Conversion and Management 105 (2015) 393–402

Contents lists available at ScienceDirect

Energy Conversion and Management

journal homepage: www.elsevier.com/locate/enconman

Evaluation of the thermal efficiency and a cost analysis of different types of ground heat exchangers in energy piles

Seok Yoon [a], Seung-Rae Lee [a,*], Jianfeng Xue [b], Kai Zosseder [c], Gyu-Hyun Go [a], Hyunku Park [d]

[a] Department of Civil and Environmental Engineering, KAIST, Daejeon 305-701, South Korea
[b] School of Applied Sciences and Engineering, Federation University Churchill, 3842 VIC, Australia
[c] Hydrogeology and Geothermal Energy Group, TUM, Arcisstr. 21, Munich, Germany
[d] Civil and Infrastructure Business Unit, Samsung C&T Corporation, Seoul 137-956, South Korea

ARTICLE INFO

Article history:
Received 28 April 2015
Accepted 2 August 2015

Keywords:
Energy pile
Thermal performance test
Heat exchange rate
Cost analysis

ABSTRACT

This paper presents an experimental and numerical study of the results of a thermal performance test using precast high-strength concrete (PHC) energy piles with W and coil-type ground heat exchangers (GHEs). In-situ thermal performance tests (TPTs) were conducted for four days under an intermittent operation condition (8 h on; 16 h off) on W and coil-type PHC energy piles installed in a partially saturated weathered granite soil deposit. In addition, three-dimensional finite element analyses were conducted and the results were compared with the four-day experimental results. The heat exchange rates were also predicted for three months using the numerical analysis. The heat exchange rate of the coil-type GHE showed 10–15% higher efficiency compared to the W-type GHE in the energy pile. However, in considering the cost for the installation of the heat exchanger and cement grouting the additional cost of W-type GHE in energy pile was 200–250% cheaper than coil-type GHE under the condition providing equivalent thermal performance. Furthermore, the required lengths of the W, 3U and coil-type GHEs in the energy piles were calculated based on the design process of Kavanaugh and Rafferty. The additional cost for the W and 3U types of GHEs were also 200–250% lower than that of the coil-type GHE. However, the required number of piles was much less with the coil-type GHE as compared to the W and 3U types of GHEs. They are advantageous in terms of the construction period, and further, selecting the coil-type GHE could be a viable option when there is a limitation in the number of piles in consideration of the scale of the building.

1. Introduction

Among various renewable energy resources, geothermal energy has been regarded as one of the most environmentally friendly and efficient types for space heating and cooling [1–3]. Geothermal energy has great potential as a directly usable type of energy, especially in conjunction with ground-source heat pump (GSHP) systems. Therefore, GSHP systems combined with various types of ground-heat exchangers (GHEs) are widely used [4–7].

The main elements of a GSHP system are the geothermal heat pump and the GHE. Geothermal energy can be obtained through GHEs. With geothermal cooling/heating systems, heat energy is fed into and withdrawn from the ground via GHEs [8–10]. The GHE extracts heat from or injects it into a circulation fluid (e.g., water or an anti-freeze solution) flowing through the GHE. Conventional vertical GHEs consist of U- or W-shaped GHEs inserted into a borehole. However, a conventional vertical GSHP system has a high initial cost for the required drilling. As an alternative, a GSHP with an energy pile foundation has recently been developed and used. With this system, the GHEs are embedded into a cast-in-place grout pile [11–14]. Fig. 1 illustrates the concept of the conventional vertical GHE and the energy pile [15]. The energy pile is generally shorter by several tens of meters. In Korean practices, PHC piles are broadly used. Moreover, to compensate for the shallow installation depth of the energy pile, spiral coil-type GHEs can be used to enhance the heat efficiency because they can increase the heat exchange area compared to U-type GHEs [13,15,16].

Although there have been many researches of energy piles, a few have conducted thermal efficiency analyses despite the fact that an energy pile is known to reduce the installation cost and offer a viable compromise between an increase in the efficiency

* Corresponding author at: Department of Civil and Environmental Engineering, KAIST, 291, Gwahakro, Yuseong-gu, Daejeon 305-701, South Korea. Tel.: +82 42 350 3617; fax: +82 42 350 7200.
E-mail address: srlee@kaist.ac.kr (S.-R. Lee).

http://dx.doi.org/10.1016/j.enconman.2015.08.002
0196-8904/

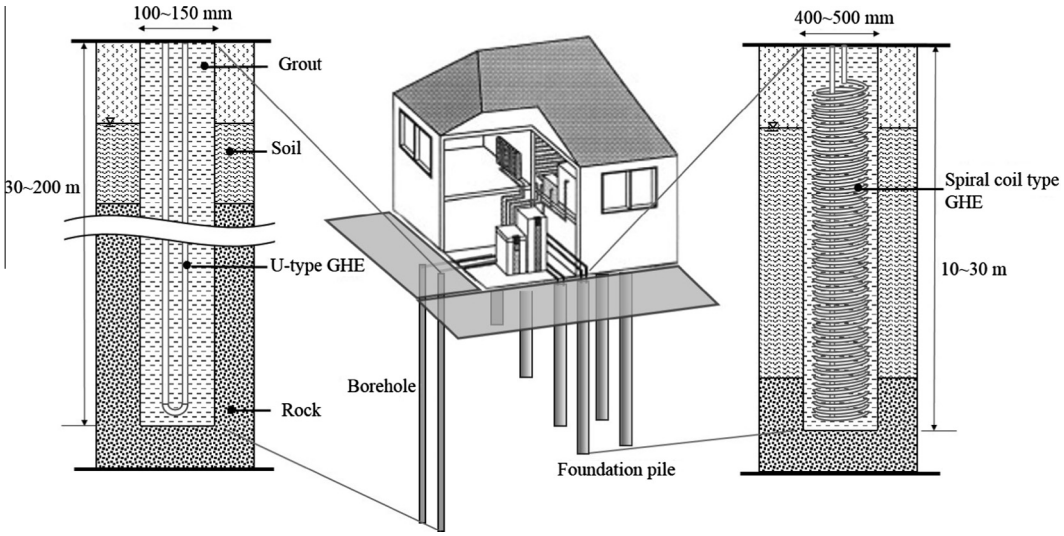

Fig. 1. Schematic diagram of a vertical borehole and an energy pile [15].

and the cost [17–19]. Furthermore, there have been a few researches which describe thermal efficiency evaluation among different kinds of GHEs in energy pile.

Therefore, this paper presents the results from an experimental and numerical study with finite element method programs such as ABAQUS Standard and COMSOL Multiphysics [20] by comparing the heat exchange rates using a precast high-strength concrete (PHC) energy pile with W and coil-type GHEs (Fig. 2) installed at an electric substation in Suwon, which is in the northwestern corner of South Korea. In addition to calculating the heat exchange rate, a cost-efficiency analysis was also conducted in order to evaluate optimal thermal efficiency of each type GHEs based on the whole construction cost.

2. Experimental setup

2.1. Setup of energy pile

PHC piles using coil and W-type GHEs were installed to construct an energy pile. Table 1 summarizes the dimensions of the energy pile and the GHEs. Polybutylene pipes (inner/outer diameter of pipe = 0.016/0.02 m) were used as the GHEs; they had a coil pitch of 5 cm. Cement grout with a cement-to-water ratio of 0.5 was poured and cured for about 28 days [20]. Fig. 3 shows the construction process of the energy pile. Since the TPT can consider only cooling operation mode, the inlet temperature was set 30 °C during the TPT (thermal performance test) as it is normally around

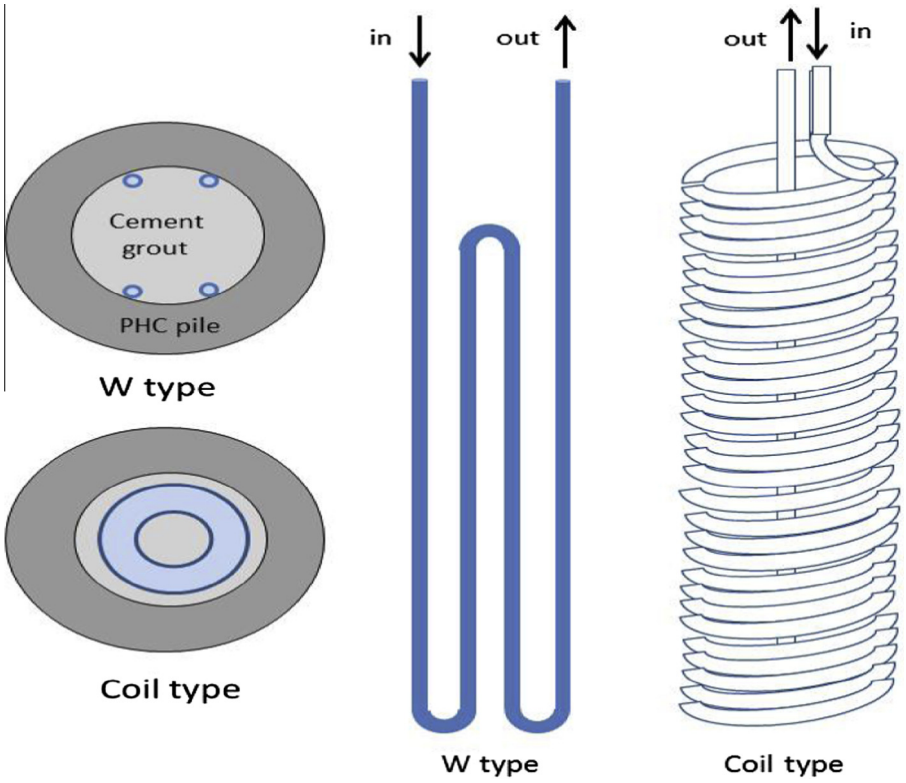

Fig. 2. Diagram of the energy piles.

Table 1
Specifications of the energy piles.

Dimension of piles	Coil	W
Pile depth (m)	12.8	13.27
Pile inner diameter (mm)	245	225
Pile outer diameter (mm)	400	400

30 °C in summer, especially in Korea. The resistance temperature detector sensors were attached to the inlet and outlet of the pipes to measure the circulating water temperature.

The ground was composed of weathered granite soil and stiff weathered rock. Ground water level was 4.5 m below from the top of energy pile and no ground water flow was observed. Average void ratio e and water content w of the weathered granite soil below and above the ground water table were measured as follows: $e = 0.66$, $w = 12.4\%$ above ground water level, and $e = 0.45$, $w = 16.7\%$ below ground water level. The ground thermal conductivity was measured using TP-02 device (Hukseflux Thermal Sensors Inc, Delft, Netherlands) based on a transient hot-wire method [21,22]. Soil was remolded in an indoor laboratory to ensure the same void ratio and water content of the construction site. The thermal conductivities of the soils above and below the ground water table were measured and determined to be 1.1 and 2.4 W m^{-1} K^{-1}, respectively.

2.2. Theory of TPT analysis

The heat transfer process of the GHE is related to the absorption and release of heat to and from the borehole and ground as the heat transfer fluid flows through the GHE within the borehole [14,23]. The heat exchange rate of energy pile between the GHE and the surrounding medium can be measured by means of a TPT. Generally, the thermal response test (TRT) can be applied to measure the ground thermal conductivity using a line source or cylindrical source model while supplying constant power to the TRT equipment [24–26]. On the other hand, the TPT can be used to measure the heat exchange rate of the GHE under the condition that the inlet temperature is kept constant [17]. The heat exchange rate per pile depth (q) was calculated using Eq. (1).

$$q = mc(T_{in} - T_{out})/L \tag{1}$$

Here, T_{in} is the inlet temperature of the fluid (K), T_{out} is the outlet temperature of the fluid (K), m is the flow rate of the fluid (kg s^{-1}), c is the specific heat capacity of the fluid (J kg^{-1} K^{-1}), and L is the pile depth (m). The TPT equipment in this research can also be used to conduct a TRT, as it is equipped with a heater controller as well as a temperature controller. In other words, this equipment is capable of conducting both a TRT and TPT.

3. Numerical analysis

In this study, the TPTs were numerically simulated using a conductive heat transfer analysis scheme implemented in ABAQUS/Standard [27] with the user subroutine method and COMSOL/Multiphysics [28], coupled with a computation fluid dynamics (CFD) analysis. The conjugate heat transfer behaviors were simply modeled based on the following assumptions: convective heat transfer between the circulating fluid and pipe, conductive heat transfer in the grout, and conductive heat transfer in the soil [20,29]. Generally, heat transfer in a normal unfrozen soil is mainly governed by conduction, while radiation and convection can be regarded to be insignificant if there is negligible ground water flow [20,30]. The heat transfer governing equation from conduction in the ground is as follows:

$$\lambda_i\left(\frac{\partial^2\theta_i}{\partial r^2}+\frac{1}{r}\frac{\partial\theta_i}{\partial r}+\frac{\partial^2\theta_i}{\partial z^2}\right)+Q_{\text{int}}=\rho_i c_i\frac{\partial\theta_i}{\partial t} \tag{2}$$

In this equation, the subscript i denotes the material, θ is the temperature variation (K), t is time, λ is the thermal conductivity (W m^{-1} K^{-1}), ρ is the density (kg m^{-3}), c is the specific heat capacity (J kg^{-1} K^{-1}), r is the radial distance, and z is the longitudinal distance, and Q_{int} is the internal heat generation (W m^{-3}).

3.1. Heat transfer analysis of a W-type GHE

Choi et al. [29] developed a three-dimensional transient conductive heat transfer model and considered an intermittent operation condition by modeling a forced convective heat boundary condition that represented the convective heat transfer of the circulating fluid. The heat transfer mechanism of line-type GHEs similar to the W-type was introduced in earlier works [20,29]. The ABAQUS/Standard program with the aforementioned three-dimensional transient conductive heat transfer model [29] was used for the simulation of the W-type GHE.

3.2. Heat transfer analysis of a coil-type GHE

As illustrated in Fig. 4, the coil-type GHE can be approximated as a series of rings placed vertically, which corresponds to an axisymmetric condition. If a uniform fluid temperature distribution is assumed in the pipe cross-section, a one-dimensional heat balance condition for two neighboring rings on an axisymmetric plane or two neighboring points along the vertical return pipe can be expressed as Eq. (3) [31].

$$\rho_f l_p c_f\frac{\partial T_{f,n+1/2}}{\partial t}+\rho_f u_f c_f[(T_{f,n+1}-T_{f,n})]=\frac{4h_{eq}l_p}{D_{in}}(T_{grout}-T_f)_{n+1/2} \tag{3}$$

(a) GHE Production (b) Insert of GHE into the pile (c) Cement grouting

Fig. 3. GHE installation in energy piles.

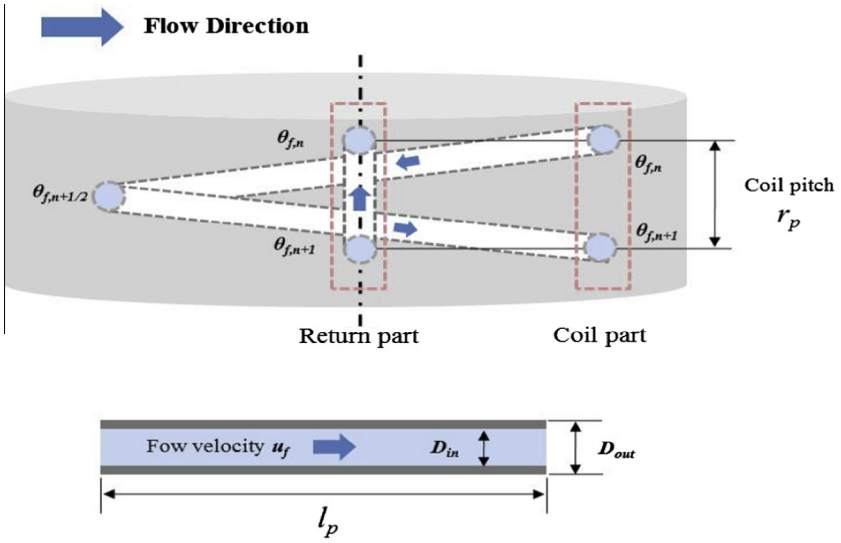

$$l_p = [(2\pi R)^2 + (r_p)^2\,]^{1/2} \text{ for coil part}$$

$$l_p = r_p \qquad \text{for return part}$$

Fig. 4. Axisymmetric model of a coil-type GHE.

where the subscript n denotes nodal position in flow direction, T_f is the bulk fluid temperature (K), T_{grout} is the grout temperature (K), ρ_f is the density of circulating fluid (kg m^{-3}), c_f is the specific heat capacity of fluid (J kg^{-1} K^{-1}), l_p is the actual flow length as described in Fig. 5 (m), D_{in} is the inner diameter of pipe (m), and h_{eq} is the equivalent convective heat transfer coefficient (W m^{-2} K^{-1}).

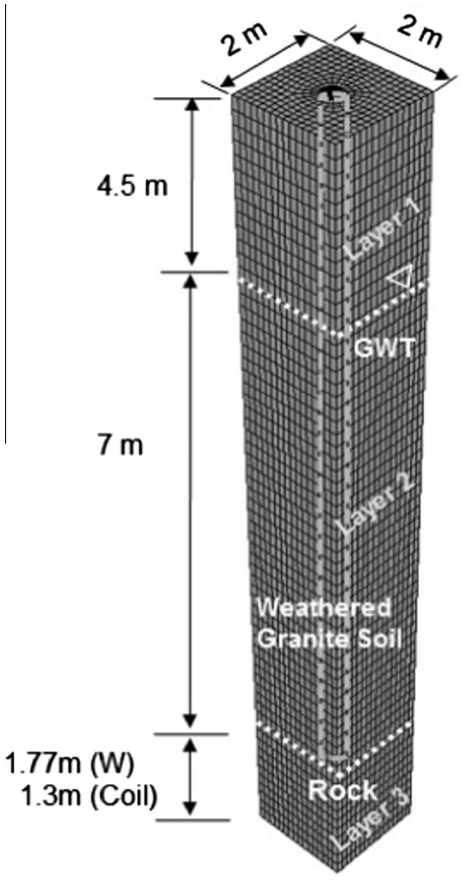

Fig. 5. Finite element model for the simulation.

By applying central implicit finite difference discretization of the space–time derivative, the one-dimensional heat balance equation can be written in an incremental form as depicted in Eq. (4). Δt is the time increment, and the subscripts n and k refer to the position in the flow direction and the time increment, respectively.

$$\begin{aligned}&\left[\rho_f u_f c_f + \frac{1}{2}\left(\frac{4h_{eq}l_p}{D_{in}} + \frac{\rho_f l_p c_f}{\Delta t}\right)\right] T^k_{f,n+1} \\ &= \left[\rho_f u_f c_f - \frac{1}{2}\left(\frac{4h_{eq}l_p}{D_{in}} + \frac{\rho_f l_p c_f}{\Delta t}\right)\right] T^k_{f,n} \\ &\quad + \frac{4h_{eq}l_p}{D_{in}}\left(\frac{T^k_{grout,n+1} + T^k_{grout,n}}{2}\right) + \frac{\rho_f l_p c_f}{\Delta t}\left(\frac{T^{k-1}_{f,n+1} + T^{k-1}_{f,n}}{2}\right)\end{aligned} \tag{4}$$

The following calculation procedure was applied in the simulation. (a) At the first increment of the operation period, the inlet temperature is assigned as the initial temperature of the fluid. (b) The conduction analysis is then performed, where the initial fluid temperature is prescribed as the sink temperature. (c) After reading the temperature of the grout nodes from the conduction analysis, the fluid temperature is recalculated using Eq. (4) in the ABAQUS user subroutine URDFLD and is reassigned as the sink temperature in the user subroutine FILM upon the next increment. This process (c) is repeated until the end of the analysis.

In addition to ABAQUS/Standard, another finite element analysis program coupled with a CFD module in COMSOL Multiphysics was used to simulate the TPT of the coil-type GHE to determine a more precise fluid flow in the coil-type GHE. The governing equation in the CFD model also considers the convective heat transfer between the circulating fluid and the pipe wall and the conductive heat transfer in the grout, pile, and soil [15]. The governing equation of the numerical model based on the convection current and conduction is expressed by Eq. (11) [32].

$$\rho_f c_f A_p u_f \cdot \nabla T = \nabla \cdot A_p \lambda \nabla T + f_D \frac{\rho_f}{2d_h}|u_f|^3 + Q + Q_{wall} \tag{5}$$

Here, Q refers to the regular heat injection ($W\,m^{-1}$) and Q_{wall} denotes the heat source, as formed through the heat exchange across the pipe wall ($W\,m^{-1}$). Q_{wall} also represents the overlap of the temperature between the fluid convection and pipe conduction. T is the temperature (K), A is the pipe cross section area (m^2), c represents the fluid specific heat capacity ($J\,kg^{-1}\,K^{-1}$), and ρ is the fluid density ($kg\,m^{-3}$). In addition, d_h is the average hydraulic diameter (m), f_D (non-dimensional) is the coefficient of friction, u_f means the tangential velocity of the fluid ($m\,s^{-1}$), and λ is the thermal conductivity ($W\,m^{-1}\,K^{-1}$). After the CFD analysis of Eq. (5), the result was coupled with the heat conduction equation of a solid mass through Eq. (6).

$$Q_{wall} = (hZ)_{eff}(T_{pipe} - T_f) \tag{6}$$

Here, T_{pipe} is the temperature of the pipe wall (K); this value comes from the heat conduction equation of the solid mass. T_f is the fluid temperature in the pipe (K). The exact heat transfer with the coupled analysis between the fluid convection and pipe conduction can be considered from Eq. (6). Furthermore, $(hZ)_{eff}$ is the effective value of the heat transfer coefficient, i.e., h ($W\,m^{-2}\,K^{-1}$) [15], multiplied by the wall perimeter Z of the pipe (m).

3.3. Finite element modeling and simulation

Fig. 5 shows the finite element model for the simulation of the TPTs; the dimensions are 10, 10, and 16 m in the x, y, and z (depth) directions. Six- and eight-node three-dimensional solid continuum elements (DC3D6 and DC3D8) for the diffusive heat transfer were used to model the grout, PHC pile, and ground in ABAQUS. The ground was divided into three regions based on a ground investigation. In COMSOL Multiphysics for the coil-type GHE, free tetrahedral meshes with a maximum element size of 1.2 m and a minimum size of 0.08 m were used. The mesh element formation of the pipe wall surface uses the wall layer built-in function of the COMSOL pipe module. The input thermal properties of the materials for the numerical simulation are presented in Table 2.

4. Results of TPTs and numerical analyses

The TPTs were performed for four days in September in 2012 with an eight-hour on and a 16-h off cycle. It is known that operation mode can affect thermal efficiency, and intermittent operation showed superior thermal performance than continuous operation mode [20,33]. Prior to TPTs, Heat-free water circulation was performed for 30 min to equalize ground and circulating fluid temperature. The initial ground temperature was 17 °C. The inlet temperature during the TPTs was kept at 30 °C to determine the cooling load condition. The average outdoor temperature during the TPT was around 30 °C. The temperatures of circulating water at the inlet and outlet were measured during the TPTs, and the flow rate of circulating water was measured at the outlet. The heat exchange rates of the coil and W-type GHE were calculated with temperature value at inlet, outlet and flow rate of circulating water using Eq. (2). Moreover, three-dimensional finite element analyses with the in-situ TPT condition were also conducted, and the results were compared with the experimental results. Fig. 6 plots the heat exchange rate of the W-type GHE and Fig. 7 compares the heat exchange rate of the coil-type GHE over a course of four days. The heat exchange rate value for each day was calculated by deriving the simple arithmetic mean of the heat exchange rates obtained from eight hours of operation. The heat exchange rate values for 3 months of operation considering cooling operation mode were also predicted by the numerical analysis. Fig. 8 shows the heat exchange rate values from the intermittent operation of the W-type GHE for three months, and Fig. 9 shows the heat exchange rate values from the intermittent operation of the coil-type GHE for three months. The results of the TPTs and the numerical analysis were in considerably good agreement, which shows that the numerical analysis model simulates the heat exchange rate values fairly well. In the coil-type GHE, two FEM models were used to simulate the TPT results. The CFD analysis with COMSOL Multiphysics showed more similar values with the TPT results than ABAQUS model, but there was not a big superiority between two FEM models. The CFD analysis was conducted for four days only for comparison purposes, as it took a considerable amount of time to describe the intermittent operation over a course of three months. When the heat exchange rates were calculated while using coil-type GHE, there were errors of approximately 10% between the results of the TPTs and the results of the numerical analysis. This likely arose due to the development of a certain degree of error in the coil-type GHE model during the numerical analysis without considering the actual irregular coil pitches and owing to differences stemming from the development of considerable head loss in the coil-type GHE in comparison with the general W-type GHE, leading to a failure to control the flow rate consistently during the TPTs.

According to the results of the TPTs and the numerical analysis, when the coil-type GHE was used for three months, the heat exchange rate per pile depth increased by approximately 10–15% in comparison with that of the W-type GHE (Table 3). This appeared to occur because when the coil-type GHE was applied, the wide heat exchange area with the grout and the ground prolonged the time during which the circulating water remained, thus increasing the amount of heat emitted to the ground. In addition, the heat exchange rate decreased with the passage of time because the ground temperature increased with time, in turn leading to a reduction in the temperature difference between the ground and the circulating water. In contrast, however, the heat exchange rate per pipe length was higher for the W-shaped heat exchangers than it was for the coil-type heat exchangers by 350–400%.

Table 2
Thermal properties of materials used in the simulation [2].

Materials	Thermal conductivity (W/m K)	Specific heat capacity (J/kg K)	Density (kg/m^3)
Soil1	1.10	1160	1800
Soil2	2.40	1280	2140
Rock	3.24	823	2640
Cement grout	2.02	840	3640
PHC	1.62	790	2700
Polybutylene pipe	0.38	525	955
Circulating water	0.57	4200	1000

5. Design approach of energy piles

5.1. Design method of the GSHP system

Eq. (1) can be converted to Eq. (7) considering the total thermal resistance in a cross-section of a GHE. The heat exchange rate per pile depth can be calculated with the temperature difference inside the mean fluid temperature (t_f) and the initial soil temperature (t_g) divided by the total thermal resistance of the GHE [34,35].

$$q = mc(T_{in} - T_{out})/L = (T_f - T_g)/\sum R \tag{7}$$

The total thermal resistance ($\sum R$) is mainly composed of the borehole thermal resistance (R_b) and the ground thermal resistance (R_g). The ground thermal resistance is calculated as a function of time, which corresponds to the time in which a particular heat

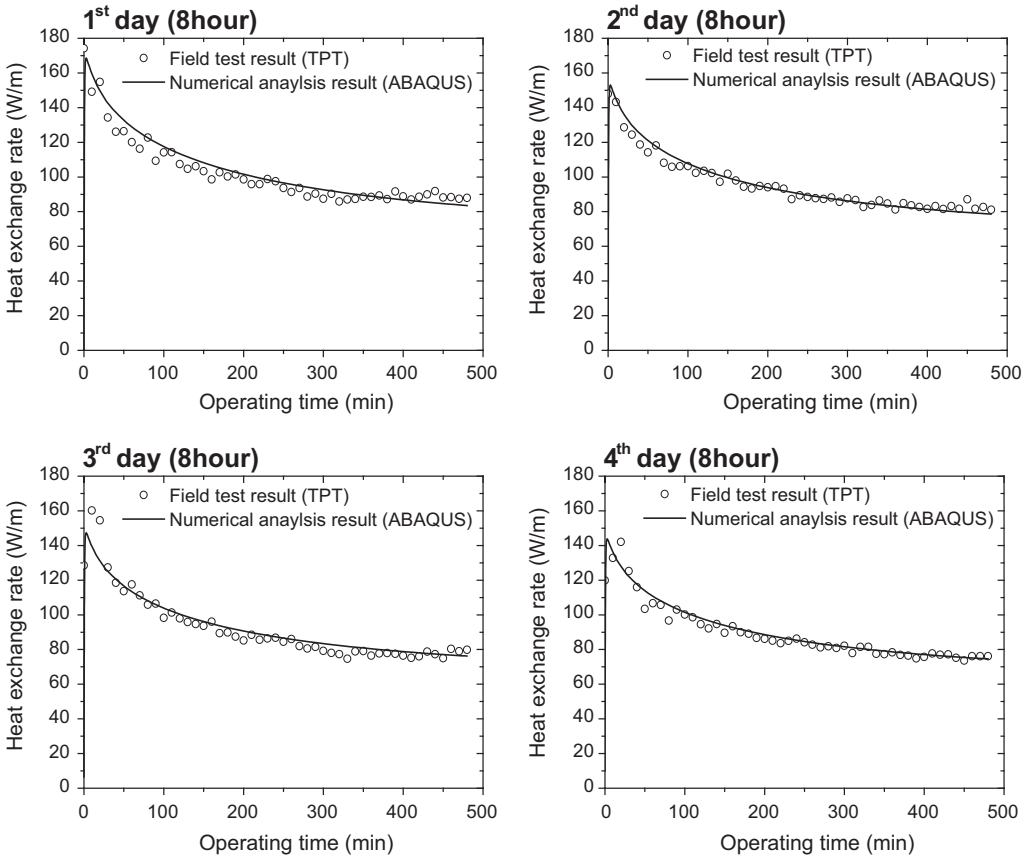

Fig. 6. Four-day heat exchange rate of the W-type GHE.

pulse occurs. Kavanaugh and Rafferty [36] applied three different heat pulses: the annual heat imbalances, the average monthly heat rates during the design month, and the maximum heat pulse for a short-term period during the design day. They then suggested design lengths of a GHE for cooling and heating, as expressed in Eqs. (8) and (9), respectively. For cooling loads, the required length is expressed as Eq. (8).

$$L_c = \frac{q_a R_{ga} + (q_{lc-} W_c)(R_b + PLF_m R_{gm} + R_{gd} F_{sc})}{T_g - \frac{T_{in}+T_{out}}{2} - T_p} \tag{8}$$

Also, for heating loads, the required length is expressed as Eq. (9).

$$L_h = \frac{q_a R_{ga} + (q_{lh-} W_h)(R_b + PLF_m R_{gm} + R_{gd} F_{sc})}{T_g - \frac{T_{in}+T_{out}}{2} - T_p} \tag{9}$$

Here, q_a represents the net annual average heat transfer to the ground, and q_{lc} and q_{lh} are the building design block loads for cooling and heating, respectively. W_c and W_h represent the power consumption of the heat pump under the designed cooling and heating loads, PLF_m is the part-load factor during the design month [36,37], and F_{sc} refers to a short-circuit heat loss factor. R_{ga}, R_{gm}, and R_{gd} represent the effective ground thermal resistances for the three different thermal pulses of the annual pulse, the monthly pulse, and the daily pulse, respectively. T_o denotes the initial ground temperature, and T_{in} and T_{out} are the fluid temperature at the inlet and outlet of the GHE. Thus, $(T_{in} + T_{out})/2$ is the mean fluid temperature of GHE. Finally, T_p is related to the long-term thermal interference effect among the adjacent piles; it is termed the temperature penalty and has a positive value for heating and a negative value for cooling [15,36].

5.2. Design results of the energy pile

In addition, reflecting the heating/cooling load of an actual industrial building in South Korea and ground conditions of the GSHP system expected to be applied, the total lengths of the energy pile were calculated with the use of the design method, as represented by Eqs. (8) and (9). In actuality, a GSHP system was not installed in this industrial building based on the exact design process. Table 4 shows a summary of the building size and building structure. 160 PHC piles were constructed as continuous footing for the foundation bearing capacity. This time, a 3U-type GHE was also considered (Fig. 9) in order to analyze various kinds of GHE types in GSHP design process of energy piles. Table 5 shows the input parameters used in the design of the energy piles. The equivalent thermal conductivity of the grout for the W-type and 3U-type GHEs were calculated by a weight equivalent formula considering the thickness of the grout and pile, as shown in Eq. (10) [2].

$$\lambda_{eq} = \frac{(r_{grout} + r_{pile})}{r_{grout}/\lambda_{grout} + r_{pile}/\lambda_{pile}} \tag{10}$$

In Eq. (10), r_{grout} is the radius of the grout (m), and r_{pile} is the outer radius of the pile (m). λ_g is the thermal conductivity of the grout (W m^{-1} K^{-1}), and λ_{pile} is the thermal conductivity of the pile (W m^{-1} K^{-1}). With the values obtained from Eq. (10), the borehole thermal resistance values for the W-type and 3U-type GHEs were calculated with multipole methods [2,38–40]. The borehole thermal resistance value of the coil type GHE was also calculated with an empirical formula developed by Go et al. [15]. Table 6 shows the design results of the energy pile. The pile depth was hypothesized to be 13.5 m considering the ground condition. When the W-type

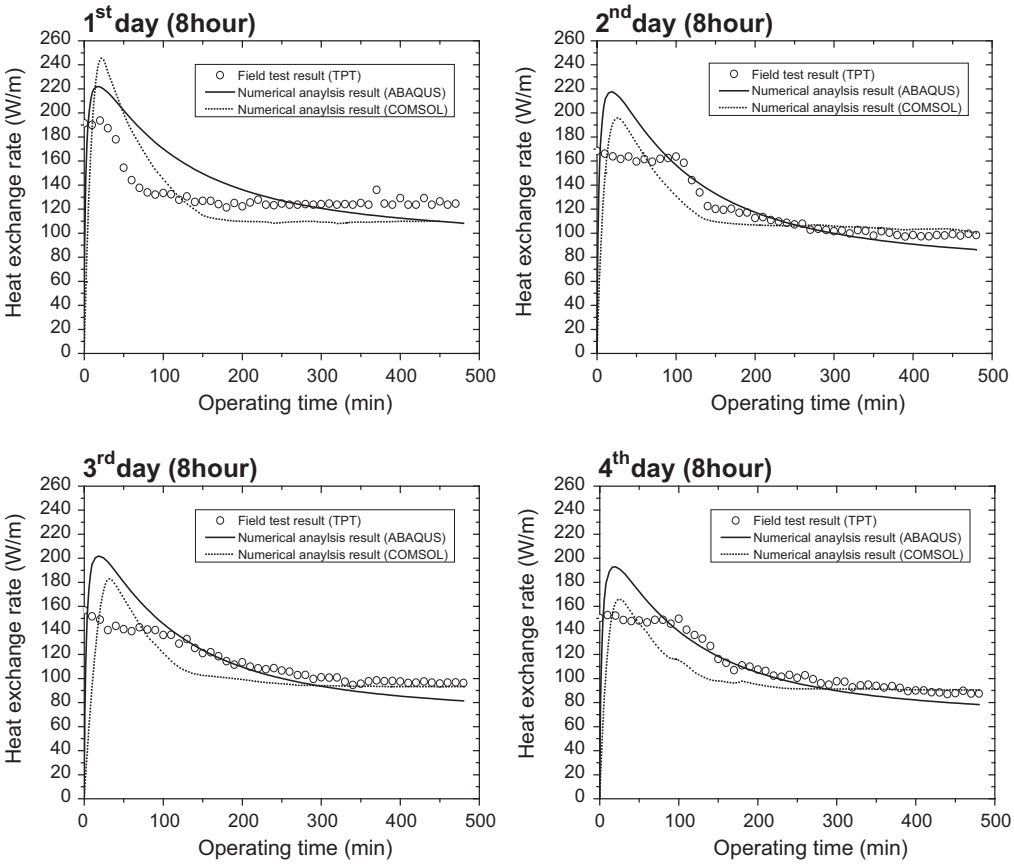

Fig. 7. Four-day heat exchange rate of the coil-type GHE.

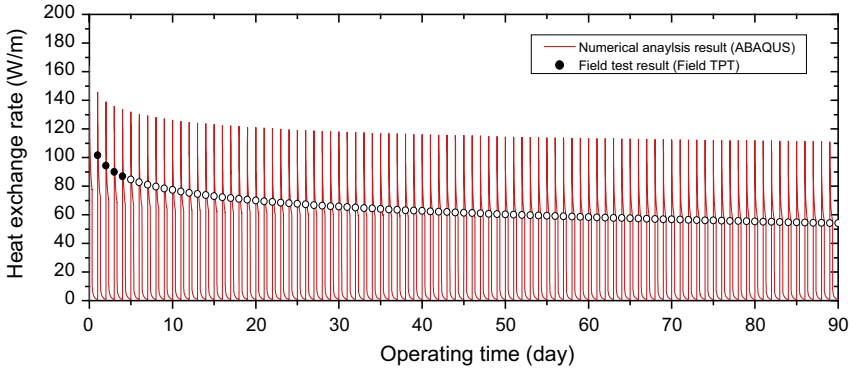

(a) W-type GHE

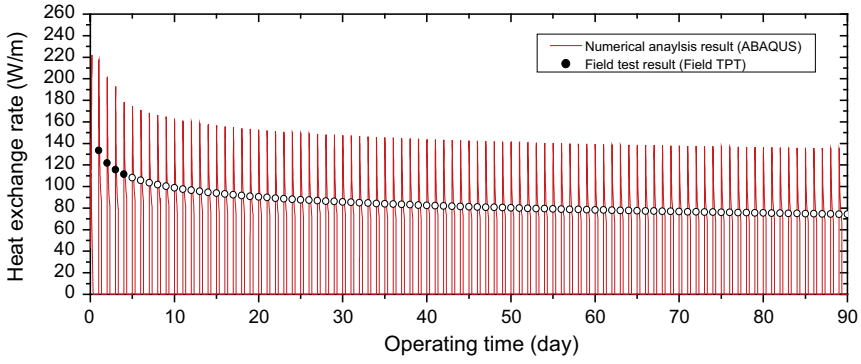

(b) Coil-type GHE

Fig. 8. Three-month heat exchange rate of GHEs for cooling operation mode.

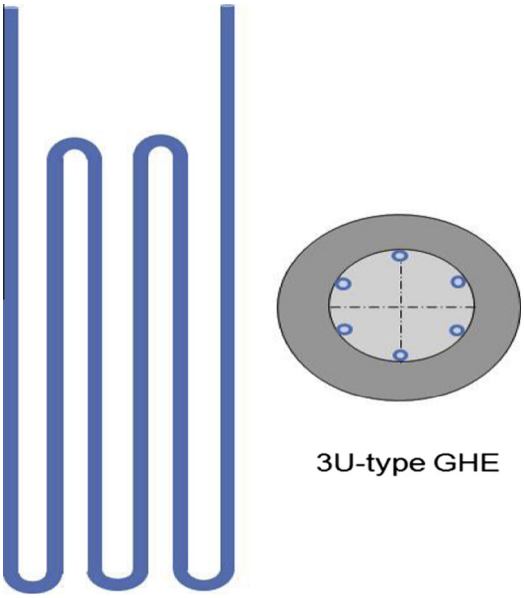

Fig. 9. Diagram of the 3U-type GHE.

and 3U-type GHEs were applied, the number of piles required increased by 20–30% in comparison with that required for the coil-type GHE.

6. Cost analysis of the energy piles

In order to analyze the costs in terms of efficiency, the lengths and number of piles necessary and the ensuing energy pile construction costs were calculated under the hypothesis that the same amount of heat, 57 kW, was emitted to the ground. First, the cost analysis was conducted using the three-month heat exchange rate values obtained by ABAQUS. According to the calculation results, coil-type GHEs required 45 piles, while W-type GHEs required 56 piles. Regarding the cost calculation, the construction costs were calculated based on South Korean standards for construction unit cost estimation and estimate prices [19,41]. Energy pile construction consists largely of pile driving, the installation of the heat exchanger, and cement grouting. The pile driving costs and pile material costs are excluded here though. When the construction costs were analyzed, a cost of approximately 7100 US dollars was calculated when W-type GHEs were applied, and a cost of approximately 21,200 US dollars was calculated when coil-type GHEs were applied. This arose most likely because the unit price of the PB pipes installed within the energy piles was more than three times higher than the cost of the pipes used in W-type GHEs, which consist of straight pipes. Moreover, the coil-type GHEs required approximately three times as many pipes as did the W-type GHEs.

Next, a cost analysis was also conducted with the results obtained from the GSHP design process shown in Table 6. Similar to the results above, when W-type GHEs and 3U-type GHEs were applied, the number of piles required increased by 20–30% in comparison with that for the coil-type GHEs, but when the W-type GHEs and 3U-type GHEs were applied, the construction costs were approximately 3 times lower in comparison with those for the coil-type GHEs. Table 7 shows a summary of the cost analysis results.

The total construction cost for this industrial building is estimated about 4,000,000–5,000,000 US dollars, and the installation costs associated with the energy pile in the GSHP system accounted for only less than one percent out of the total building construction costs, only considering the cost for the installation of the heat exchanger and cement grouting. In addition, when the coil-type GHEs were used in the energy piles, they are advantageous in terms of the construction period and interference. Especially, the application of the coil type GHE is inevitable when

Table 4
Building specifications.

Building Size	Total floor area	4,200 m^2
	Heating and cooling area	540 m^2
Cooling/heating load		121,333 kW h
Structure type		Steel frame construction

Table 5
Input parameters for the design of the energy piles.

Classification	Description
Peak load (kW)	57 (Heating & Cooling)
Annual equivalent full-load hour (h)	2129 (Heating & Cooling)
Heat pump	COP: 4.7 (Heating & Cooling) Flow rate: 11.4 (L/min)/3.5 kW
Unit inlet (°C)	Cooling: 30, Heating: 5
Ground condition	Ground temperature: 16 °C Thermal conductivity: 2.1 W/m K Thermal diffusivity: 0.08 m^2/day
Modeling time period (yr)	30
Pile size (mm)	400(outer)/240(inner)
Grout thermal conductivity (W/m K)	2.02
Pile grid arrangement	Pile depth: 13.5, pile separation: 6 m
GHE size (mm)	Polybutylene: 20(outer)/16(inner)

Table 6
Design result of the energy piles.

GHE type	W type	3U type	Coil type
Borehole thermal resistance (m K/W)	0.104	0.083	0.079
Total pile depth (m)	1186	1062	861
Number of piles	88	79	64

Table 7
Summary of the cost analysis results.

Construction cost ($)	W type	3U type	Coil type
TPT from ABAQUS	7100	–	21,200
GHSP design results	11,100	12,100	30,000

Table 3
Summary of the numerical analysis and experimental results.

GHE type		Four-day heat exchange rate (W/m)					Three-month heat exchange rate (W/m)
		1st day	2nd day	3rd day	4th day	4-day average	3-month average
W type	Experiment	102	95	92	90	95	–
	ABAQUS	104	96	93	91	97	74.8
Coil type	Experiment	134	121	115	112	120	–
	ABAQUS	137	124	116	111	123	94
	CFD	135	122	115	109	120	–

there is a limitation in the number of piles in consideration of the scale of the building. Consequently, selecting a GHE that suits the site in consideration of the scale of the building and the construction period is a viable option.

7. Conclusion

In this study, PHC energy piles were installed at a site composed of a weathered granite soil stratum. W-type and coil-type GHEs were installed, and on-site TPTs were conducted to calculate the heat exchange rates. The cooling operation conditions were hypothesized through on-site TPTs; the temperature of the circulating water injected into the ground was held to 30 °C. The TPTs were conducted for four days under the operating condition of an 8 h on and a 16 h off cycle. Next, three dimensional finite element analyses using ABAQUS and COMSOL programs were performed to simulate the TPTs in their entirety and the results were compared with the in-situ TPT results. Heat exchange rate values were also calculated for three months based on the numerical analyses. Finally, a cost analysis was conducted with the TPT results and the GSHP design procedure. The following conclusions can be derived from the results of this study.

(1) A three-dimensional finite element numerical analysis was applied to the present study and simulated the results of the TPTs comparatively accurately. For the W-type GHEs, the heat exchange rate per pile length for three months using the numerical analysis was 74.8 W/m (heat exchange rate per pipe length: 20.7 W/m). In addition, when coil-type GHEs were used for three months, the predicted value, obtained through the numerical analysis, was 94 W/m (heat exchange rate per pipe length: 6.1 W/m). Errors of approximately 10% were produced between experiments and the numerical analysis in the coil-type GHE. This was likely due to errors in the construction, in which the coil pitches failed to be maintained consistently during the actual construction and in the differences stemming from the development of considerable head loss, leading to a failure to control the flow rate consistently during the TPTs.

(2) Under the hypothesis that the same amount of heat was emitted to the ground, based on the heat exchange rate values produced, the number and costs of the necessary piles were calculated. According to the results, for the coil-type GHEs, the number of piles was the least as it showed the most superior thermal efficiency which was similar with TPT results using numerical and experimental approaches. The construction period with coil-type GHE could be reduced; the additional cost for the installation of the heat exchanger and cement grouting was approximately three times higher than W-type GHEs. In addition, adding 3U-type GHEs and reflecting the heating/cooling load of actual industrial buildings and the dimensions and ground conditions of the GSHP system, which were expected to be applied in their entirety, the pile depths and numbers demanded were calculated based on the design procedure of the GSHP system. According to the calculation results, when the W-type GHEs and 3U-type GHEs were applied, the number of piles required increased by 20–30% in comparison with that required for coil-type GHEs. However, when the W-type GHEs and 3U-type GHEs were applied, the additional costs were approximately three times lower than they were for coil-type GHEs. However, although the simple construction costs were approximately three times lower for the W-type GHEs and 3U-type GHEs, the GHE installation costs for the GSHP only accounted for an extremely small percentage of the total building construction costs. The coil-type GHEs were also advantageous in terms of the construction period. Consequently, it would be logical to select the GHE type that is adequate for the site in consideration of the scale of the building and the construction period, and be expected to show the guideline and references in selecting GHE types in energy pile from this research.

Acknowledgement

The stay of S.R. Lee and S. Yoon in Technische Universität München has been supported by the Erasmus Mundus EASED programme (Grant 2012-5538/004-001) coordinated by CentraleSupélec, and by a Regional Development Research Program (15RDRP-B076564-02) of the Ministry of Land, Infrastructure and Transport of the Korean government.

References

[1] Bayer P, Saner D, Bolay S, Ryback L, Blum P. Greenhouse gas emission savings of ground source heat pump systems in Europe: a review. Renew Sustain Energy Rev 2012;16(2):1256–67.
[2] Yoon S, Lee SR, Go GH, Jianfeng X, Park H, Park DW. Thermal transfer behavior in two types of W-shaped ground heat exchangers installed in multilayer soils. Geomech Eng 2014;6(1):79–98.
[3] Moon CE, Choi JM. Heating performance characteristics of the ground source heat pump system with energy-piles and energy-slabs. Energy 2015;81(1):27–32.
[4] Utlu Z, Aydin D, Kincay O. Comprehensive thermodynamic analysis of a renewable energy sourced hybrid heating system combined with latent heat storage. Energ Convers Manage 2014;84:311–25.
[5] Hepbasli A, Kalinci Y. A review of heat pump water heating systems. Renew Sustain Energy Rev 2009;13(6–7):1211–29.
[6] Zhang C, Guo Z, Liu Y, Cong X, Peng D. A review on thermal response test of ground-coupled heat pump systems. Renew Sustain Energy Rev 2014;40:851–67.
[7] Koohi-Fayegh S, Rosen MA. An analytical approach to evaluating the effect of thermal interaction of geothermal heat exchangers on ground heat pump efficiency. Energ Convers Manage 2014;78:184–92.
[8] Morrone B, Coppola G, Raucci V. Energy and economic savings using geothermal heat pumps in different climates. Energ Convers Manage 2014;88:189–98.
[9] Kara YA, Yuksel B. Evaluation of low temperature geothermal energy through the use of heat pump. Energ Convers Manage 2001;42(6):773–81.
[10] Koohi-Fayegh S, Rosen MA. Three-dimensional analysis of the thermal interaction of multiple vertical ground heat exchangers. Int J Green Energy 2014;12(11):1144–50.
[11] Gao J, Zhang X, Liu J, Li KS, Yang J. Thermal performance and ground temperature of vertical pile-foundation heat exchanger: a case study. Appl Therm Eng 2008;28:2295–304.
[12] Hamada Y, Saitoh H, Nakamura M, Kukbota H, Ochifuji K. Field performance of an energy pile system for space heating. Energy Build 2007;39(5):517–24.
[13] Man Y, Yang HX, Diao NR, Li X, Cui P, Fang ZH. Development of spiral heat source model for novel pile ground heat exchangers. HVAC R Res 2011;17(6):1075–88.
[14] Cecinato F, Loveridge FA. Influences on the thermal efficiency of energy piles. Energy 2015;82:1021–33.
[15] Go GH, Lee SR, Yoon S, Kang HB. Design of spiral coil PHC energy pile considering effective borehole. Appl Energy 2014;125:165–78.
[16] Li M, Lai ACK. New temperature response functions (G functions) for pile and borehole ground heat exchangers based on composite-medium line-source theory. Energy 2012;38:255–63.
[17] Gao J, Zhang X, Liu J, Li K, Yang J. Numerical and experimental assessment of thermal performance of vertical energy piles: an application. Appl Energy 2008;85:901–10.
[18] Laloui L, Moreni M, Vulliet L. Behavior of a dual-purpose pile as foundation and heat exchanger. Can Geotech J 2003;40(2):388–402.
[19] Vu NB. Life cycle cost analysis of ground-coupled heat pump systems including several types of heat exchangers. Master thesis, Korea Advanced Institute of Science and Technology, Korea; 2013.
[20] Park H, Lee SR, Yoon S, Choi JC. Evaluation of thermal response and performance of PHC energy pile. Appl Energy 2013;103:12–24.
[21] ASTM D 5334. Standard test method for determination of thermal conductivity of soil and soft rock by needle probe procedure. Annual Book of ASTM Standards. vol. 04.09; 1995. p. 225–9.
[22] IEEE Standard 442-1981. IEEE guide for soil thermal resistivity measurements. http://dx.doi.org/10.1109/IEEESTD.1981.81018.

[23] Brandl H. Energy foundations and other thermo-active ground structures. Geotechnique 2006;56(2):81–122.
[24] Florides G, Kalogirou S. First in situ determination of the thermal performance of a U-pipe borehole heat exchanger in Cyprus. Appl Therm Eng 2008;28:157–63.
[25] Shonder JA, Beck JV. Field test of a new method for determining soil formation thermal conductivity and borehole resistance. ASHRAE Trans 1999;106:843–50.
[26] Pahud D, Matthey B. Comparison of the thermal performance of double U-pipeborehole heat exchangers measured in situ. Energy Build 2001;33:503.
[27] ABAQUS Inc., ABAQUS user's manual Ver. 6.5, Rhode Island; 2004.
[28] Comsol Inc., Comsol multiphysics user's manual Ver. 4.3a. USA; 2012.
[29] Choi JC, Lee SR, Lee DS. Numerical simulation of vertical ground heat exchangers: intermittent operation in unsaturated soil condition. Comput Geotech 2011;38:949–58.
[30] Rees SW, Adjail MH, Zhou Z, Davies M, Thomas HR. Ground heat transfer effects on the thermal performance of earth-contact structures. Renew Sustain Energy Rev 2000;4(3):213–65.
[31] Nakayama A, Kuwahara F, Kokubo N, Ishida T, Ohara N. A numerical model for thermal systems with helically-coiled tubes and its experimental verification. Heat Mass Transfer 2002;38:389–98.
[32] Incropera FP, Burkhard S. Fundamentals of heat and mass transfer. 4th ed. John Wiley and Sons; 1996.
[33] Jalaluddin, Miyara A. Thermal performance investigation of several types of vertical ground heat exchangers with different operation mode. Appl Therm Eng 2012;33–34:167–74.
[34] Ingersoll LR, Zobel OJ, Ingersoll AC. Heat conduction: with engineering and geological applications. New York: McGraw-Hill; 1954.
[35] Jun L, Xu Z, Jun G, Jie Y. Evaluation of heat exchange rate of GHE in geothermal heat pump systems. Renew Energy 2009;34:2898–904.
[36] Kavanaugh SP, Rafferty K. Ground-source heat pumps: design of geothermal systems for commercial and institutional buildings. Atlanta: ASHRAE, Inc.; 1997.
[37] Kavanaugh SP. Simulation and experimental verification of vertical ground coupled heat pump systems. Ph.D. Dissertation, Oklahoma State Univ; 1984.
[38] Bennet J, Claesson J, Hellstrom G. Multipole method to compute the conductive heat flows to and between pipes in a composite cylinder. Heat Transf 1987:3 [Lund University, Lund, Sweden].
[39] Young TR. Development, verification and design analysis of the borehole fluid thermal mass model for approximation short term borehole thermal response. Master Thesis, Oklahoma State Univ; 2004.
[40] Hu P, Yu Z, Zhu N, Lei F, Yuan X. Performance study of a ground heat exchanger based on the multipole theory heat transfer model. Energy Build 2013;65:231–41.
[41] Korean Institute of Civil Engineering and Building Technology (KICT). Korean standard of estimate on civil construction; 2014.